Dissociative versus molecular adsorption of phenol on Si(100)2×1: A first-principles calculation

Marilena Carbone,[1] Simone Meloni,[2] and Ruggero Caminiti[3]
[1]*Dipartimento di Scienze e Tecnologie Chimiche, Università di Roma Tor Vergata, via della Ricerca Scientifica 1, 00133 Rome, Italy*
[2]*Consorzio Interuniversitario per le Applicazione di Supercalcolo Per Università e Ricerca, via dei Tizii 6/b, 00185 Rome, Italy*
[3]*Dipartimento di Chimica, Università di Roma "La Sapienza," Piazzale Aldo Moro 5, 00185 Rome, Italy*
(Received 3 August 2006; revised manuscript received 15 May 2007; published 20 August 2007)

We investigated the competitive adsorption of a bifunctional molecule, phenol, on Si(100)2×1 by *ab initio* calculations. We performed geometry optimizations of phenol adsorbed either molecularly or dissociatively, on five possible sites (top, bridge, valley bridge, cave, and pedestal), in the low coverage regime. We found that the dissociative adsorption of phenol on top of a silicon dimer is the most favorable adsorption configuration. In the group of dissociative adsorption the phenol initially placed on the bridge or the valley-bridge sites ends up as a toplike local minima. The pedestal and cave sites remain as low-adsorption energy "open" sites. In the group of molecular adsorption, a higher adsorption energy is associated to the adsorption through an addition reaction and loss of the aromatic character (bridge, valley-bridge, and pedestal sites). Standard butterfly or diagonal butterfly are the corresponding optimized geometries. Retention of aromatic character and lower adsorption energy are associated to the adsorption on the top and cave sites. The ordering of adsorption sites according to the adsorption energy shows a mixture of the dissociative and the molecular sites. In the case of adsorption on the top site, the adsorption energies after a rotation of the phenoxy fragment along the bonding axis and hydrogen migration on the surface are very similar. The bend of the phenoxy fragment on the surface, instead, is not favored (the adsorption energy is 1.004 eV lower compared to the vertical position). Different electron density maps were calculated for different adsorption sites and modes. Finally, we investigated the possibility that molecularly adsorbed phenol behaves as a precursor for the dissociative one by nudged elastic band calculations. We found a barrier of the same order of magnitude of the thermodynamic energy at room temperature for the conversion of the valley-bridge molecular into the top dissociative site.

DOI: 10.1103/PhysRevB.76.085332 PACS number(s): 68.43.Bc

I. INTRODUCTION

The adsorption of simple organic molecules on silicon has been long studied both from an experimental[1–10] and from a theoretical point of view.[11–21] A recent development in the adsorbate-silicon systems was the investigation of multifunctional molecules which may be employed in stepwise reactions, where in the first step the molecule anchors to the surface with one functional group and in a following step it may interact with an incoming reactant.

In order to define a system with such properties several parameters need to be evaluated, such as the number and type of functional groups, their mutual position and, as a consequence, if they are attached to a rigid frame like an aromatic ring or a more mobile one like an aliphatic chain. An example of a multifunctional molecule adsorbed on a surface is geranyl-acetone (an 11C-atoms alkyl chain with two double bonds and one ketone function) on Si(111)7×7.[22] By combined experimental techniques it was established that the carbonilic oxygen binds to the rest atoms and the double bonds may interact with the adatoms as well. The molecule is probably folded onto the surface.

Other examples of bifunctional molecules investigated either experimentally or theoretically are toluene on Si(100)2×1,[23,24] and 1,2- or 1,4-dichlorobenzene on Si(100)2×1.[25] In both cases the alternative reactions, i.e., molecular or dissociative, were considered. In the former case the hydrogen extraction from the methyl substituent was found to be the most likely reaction pathway. The reaction of chlorinated molecules on Si(100)2×1 is related to the adsorption mode. The on-top adsorption leads to a configuration that preserves the C-Cl bonds at the expense of the aromatic character of the ring. At variance with this behavior, the in-between-rows adsorption occurs via C-Cl bond cleavage and preservation of the aromatic character of the ring.

In this paper, we present a theoretical investigation of the bifunctional molecule phenol on Si(100)2×1. The two functional groups interact with the surface in different ways, i.e., the hydroxyl group and the aromatic ring may give rise to a dissociative and a molecular adsorption, respectively. Photoemission experiments of phenol on Si(100)2×1 showed a dissociative adsorption with the OH cleavage and the creation of Si-OPh and Si-H bonds.[26]

The adsorption of phenol on Si(111)7×7, instead, is coverage dependent.[27] At low coverages, the dissociative adsorption prevails and occurs on surface rest atoms, at higher coverages the adsorption becomes molecular and occurs on adatoms.

The variety of phenol adsorptions on Si(111)7×7 induced us to perform more investigations also on Si(100)2×1. Therefore, we made a systematic theoretical investigation on the dissociative and molecular adsorption of phenol on the five possible adsorption sites of Si(100)2×1: top, bridge, cave, pedestal, and valley bridge (T,B,C,P,V).

Furthermore, we evaluated the possible hydrogen migration and the bending of the phenoxy fragment towards the surface upon dissociation.

Finally, we considered the kinetic aspects of the adsorption process. We found that the dissociative adsorption is energetically more favorable than the molecular one. By using the climbing image nudged elastic band method, we checked whether a molecular adsorbate could act as a precursor of a dissociative one.

II. METHOD

We performed *ab initio* calculations within the framework of the density functional theory using gradient corrections in the Becke-Lee-Yang-Parr implementation[28] and expanding Kohn-Sham orbitals on a plane wave basis set. We adopted the CPMD code[29] for the geometry optimizations and Quantum Espresso for probing a reaction pathway by nudged elastic band (NEB).[30] The accuracy in the description of the chemical processes on silicon surface has been shown to improve with respect to the pure local density approximation when gradient corrected functionals are adopted.[31,32] The calculations have been carried out using norm-conserving Trouiller-Martins pseudopotentials.[33]

We expanded the wave functions in plane waves up to an energy cutoff of 60 Ry. We checked that the structural and binding properties of the systems are all well converged at this value.

The calculations were performed under periodic boundary conditions with the periodically repeated unit cells referred to as supercells. A surface model is built with $Si_{72}H_{12}$ corresponding to six layers of Si atoms and six surface dimers. This surface size allows the optimization of the phenol position, including the flat ones on all possible surface sites.

The silicon layers were included in this supercell with vacuum regions of about 14 Å in the [001] direction (2 times as much as the crystal dimension in the [001] direction, while keeping the periodicity in the [100] and [010] directions). The large vacuum region allows the geometry optimization both when the phenol molecule lies perpendicular to the surface, hence avoiding interference of other images. We adopted a sampling of the Brillouin zone at the Γ point, similarly to the cases of ethanol,[18] methanol,[21] toluene,[24] and stilbene[34] on Si(100). A monolayer of hydrogen is used to saturate the dangling bonds on the lower side of the slab.

The reliability of the approach has been probed by calculations of the gas-phase phenol molecule, in identical conditions as the adsorbate models, i.e., with a supercell of identical size and same vacuum region, cutoff, and potential. The results were compared to the phenol geometry obtained using the restricted Hartree-Fock level of theory and the second-order Møller-Plesset formalism.[35] We found an average C-C bond length of 1.395 Å, to be compared to 1.384 Å obtained by Gadosy and McClelland.[32]

We optimized the geometry of the Si surface starting from symmetric dimers and allowing the first two layers to fully relax. The others were fixed in order to mimic the bulk. The output geometry was the well-known model with asymmetric dimers.

We found that the dimer bond length is 2.25 Å and the buckling angle of 19° is in agreement with the reconstruction calculated by Krüger and Pollmann.[36]

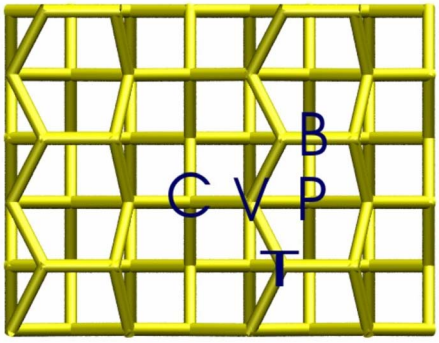

FIG. 1. (Color online) A sketch of the Si(100)2×1 surface. Six asymmetric dimers are employed. Five possible adsorption sites are marked: *T* (top), *B* (bridge), *C* (cave), *V* (valley-bridge), and *P* (pedestal). The plots are made with the aid of the visual molecular dynamics program (Ref. 38).

Also for the adsorbate-substrate systems, all geometrical parameters of the top two layers of Si as well as the adsorbate, were allowed to fully relax.

Adsorption energies are calculated as the difference between the energy of an optimized model and the separate phenol and silicon moieties. The numerical values are, then, reported with inverted signs. Different electron density maps were calculated for the most representative dissociative and molecular adsorption sites, in order to get a better insight in the adsorption process.

The energy barrier for the transition from a sample molecular to a dissociative adsorption site was calculated by NEB, after making sure we obtained the same adsorption energies for the selected systems with the two codes using the same functionals and pseudopotentials.

III. RESULTS AND DISCUSSION

Phenol may interact with the silicon surface according to three reaction mechanisms: the addition and the substitution reactions on the aromatic ring and the cleavage of the O-H bond. In the addition reaction the reactant (in this case a silicon atom) binds directly to a C atom, without cleavage of the C-H, hence with loss of the aromatic character and of the flat geometry. The second type of reaction, i.e., the substitution, occurs with a cleavage of the C-H bond and was discarded as unlikely, since there is no experimental evidence. Furthermore, also for a similar system, i.e., toluene (methylbenzene) on the same surface there is no evidence of substitution on the ring, but on the methyl group.[37] The third type of reaction is just the cleavage of the O-H bond and the formation of a Si-O bond, to yield a silicon-phenoxy unit.

In the following sections we will consider two adsorption types, the molecular one, which may include the addition reaction, and the dissociative one, that occurs through the O-H cleavage. Each of those adsorption types has been calculated for each of the possible adsorption sites on the Si(100)2×1 surface (shown in Fig. 1).

A. Molecular models

The molecular models were built by centering the aromatic ring on the chosen adsorption site at 2 Å from the plane of the up atoms of the dimers.

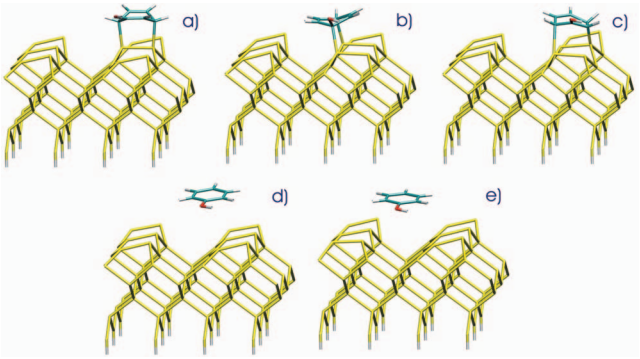

FIG. 2. (Color online) Optimized geometries of phenol molecularly adsorbed on different Si(100)2×1 surface sites. The models are ordered according to their increasing binding energy: (a) starting bridge site ending with a standard butterfly on a single dimer, (b) starting valley-bridge site ending with a standard butterfly on two dimers upon optimization, (c) starting pedestal site ending with a diagonal butterfly upon optimization, (d) top site, and (e) cave site.

Upon geometry optimization, we obtained two subgroups of molecular adsorbates, those which retain the aromatic character (A group) and the ones which undergo an addition reaction and, as a consequence, loose the aromatic character (NA group). Also bond lengths and electron density distribution are different for the two groups and make the phenyl ring more similar to a cyclohexadiene in the latter case.

The addition reaction occurs when phenol is initially on a bridge, valley-bridge, and pedestal site. The adsorption on the top and cave sites preserves the aromatic character.

The outcomes of the geometry optimizations for the molecular models are reported in Fig. 2, the adsorption energies and geometrical parameters are reported in Tables I and II, respectively. In general, the NA group has lower binding energies than the A group. The ordering of the sites according to their decreasing adsorption energy is $B_m > V_m > P_m > T_m > C_m$.

The silicon surface is affected by the adsorption process in a different way in the two subgroups. The silicon atoms belonging to the dimer participate to the addition reaction, with consequent unbuckling. At variance with this behavior, the dimers stay buckled when a weak interaction between the ring and the surface occurs and phenol remains aromatic.

The geometrical outcome when phenol is initially placed on a bridge or a valley-bridge site is a standard butterfly [Figs. 2(a) and 2(b)]. The adsorption initially on a pedestal site yields a diagonal bridge geometry [Fig. 2(c)]. In these configurations the phenol is converted into a 1hydroxyl-2,5-cyclohexediene or a 1hydroxyl-1,4-cyclohexediene, depending on the position of carbon atoms attached to the silicon surface, with respect to the hydroxyl groups. The adsorption energies are 0.551 eV, 0.262 eV, and 0.203 eV, respectively. The smaller energy for the initial valley-bridge compared to the bridge site, in spite of the similar final configuration, is probably related to the energy loss due to the unbuckling of two dimers in the former case instead of one as in the latter case. For the standard butterfly configurations the Si-C bond lengths are of order of 2 Å and the residual dimer buckling is $<5°$.

TABLE I. Adsorption energies calculated for the various phenol adsorption sites on Si(100)2×1. Top rot is the top site with the phenol 90° rotated with respect to the dimer axis. Top rot swap is the top site with the phenol 90° rotated and originally positioned on the up atom of the silicon dimer.

Molecular adsorption	Adsorption energy (eV)
Bridge	0.551
Valley bridge	0.262
Pedestal	0.203
Top	0.073
Cave	–0.494
Dissociative adsorption	**Adsorption energy (eV)**
Top	2.522
Top rot	2.560
Top rot swap	2.557
Tilted	1.517
H	2.495
Bridge	2.473
Valley bridge	1.677
Pedestal	0.478
Cave	0.051

The diagonal bridge configuration is strongly asymmetric, with the four shortest Si-C distances at 2.13, 2.15, 2.21, and 3.12 Å. The residual buckling is also different for the two silicon dimers involved in the bonds, 5.9° for the first and 13.6° for the second.

Phenol on the top and cave sites preserves the aromatic character [Figs. 2(d) and 2(e)]. The corresponding adsorption energy is either very small (top site) or negative (cave site). Hence, in these configurations phenol is very weakly bonded. This could be expected for the cave site, since it is an "open" adsorption site. For the top site, the weak interaction may be related to relative phenol-surface geometry that exposes a silicon atom of the dimers to the center of the ring, which has a low electron density.

B. Dissociative models

In the initial models for the dissociative adsorption, the phenoxy fragment was positioned on the chosen site and the hydrogen on the same or on the closest dimer, on top of one silicon atom. Both fragments were initially at 2 Å.

The ordering of the sites according to their decreasing adsorption energy is $T_d > B_d > V_d > P_d > C_d$. The outcomes of the geometry optimizations for the dissociative models are reported in Fig. 3. Adsorption energies and geometrical parameters are reported in Tables I and II, respectively.

The top site [Fig. 3(a)] is the most favorable one for the dissociative phenol adsorption, with an adsorption energy of 2.522 eV (2.560 eV when it is rotated along the C-O bond). The calculated distances are 1.68 Å for Si-O and 1.38 Å for C-O, and the Si-O-C angle is 149.1°. The residual dimer buckling is 5.2°.

TABLE II. Geometrical parameters: bond lengths, dimer buckling, and bond angles for the various molecular and dissociative adsorption sites. Top rot is the top site with the phenol 90° rotated with respect to the dimer axis. Top rot swap is the top site with the phenol 90° rotated and originally positioned on the up atom of the silicon dimer. In the case of the molecular adsorption on the top site the shortest Si-C distances are reported. The reported buckling angles refer to the dimers involved in the bond with phenol, or the closest silicon dimers, in case of adsorption with retention of the aromatic character. The character (H) indicates the dimer bearing the hydrogen atom. SB and DB are the standard butterfly and the diagonal butterfly, i.e., the final geometries.

Molecular adsorption	Si-C (1)	Si-C (2)	Dimer buckling (1)	Dimer buckling (2)	Dimer buckling (3)	Dimer buckling (4)
Bridge (SB)	2.00(1)	1.99(1)	2.4°			
Valley bridge (SB)	1.97(0)	1.98(8)	4.2°	0.6°		
Pedestal (DB)	2.13(0)	2.15(2)	5.9°			
	2.21(9)	3.12(1)				
Top	3.16(3)		21.8°	19.9°	21.6°	19.5°
	3.47(0) 3.53(9)					
Dissociative adsorption	**Si-O**	**O-C**	**Dimer buckling**	**Dimer buckling (H)**	**Angle Si-Ô-C**	
Top	1.68(2)	1.38(5)	5.2 °		149.10°	
Top rot	1.68(6)	1.38(8)	3.3°		144.78°	
Top rot swap	1.68(9)	1.39(0)	0.5°		146.94°	
Tilted	1.69(9)	1.39(2)	1.4°		156.96°	
H	1.69(5)	1.38(5)	2.6°	4.8°	143.86°	
Bridge	1.68(6)	1.38(6)	6.5°	3.8°	145.79°	
Valley bridge	1.77(2)	1.41(0)	1.0°		147.23°	
	3.43(7)					
Pedestal	2.80(0)–2.90(2)	1.34(1)	16.7 °	2.4°		
	2.90(5)–2.74(4)					
Cave	3.47(3)–3.40(7)	1.29(1)	21.6°			
	3.78(9)–3.56(1)					

The adsorption of phenol initially on the bridge site yields a final toplike geometrical configuration [Fig. 3(b)]. The Si-O bond distance is the same as for the top site, the Si-O-C angle is slightly smaller (145.8°), and the residual buckling of the silicon dimer is 6.5°. The adsorption energy, 2.473 eV, is also very close to the adsorption on the top site. The small energy difference between the two models is related to the binding of the hydrogen atom to a neighboring dimer, instead of the same dimer as for the top site. We tested this hypothesis running a calculation of a model where the phenoxy and the hydrogen fragments are placed on two neighboring dimers from the start. We obtained the same configuration [Fig. 4(d)] with the same energy (see Table I) as for the initial bridge site.

In the valley-bridge model the oxygen of the phenoxy fragment is initially positioned equally distant from the silicon atoms of two dimers of two parallel rows [Fig. 3(c)]. These distances become nonequivalent and the model more similar to a top site. At convergence, one distance becomes 1.77 Å and the other one 3.44 Å. Also the C-O bond is slightly stretched, compared to the top site (1.41 Å vs 1.38 Å). Only one of the two dimers initially involved in the binding process becomes symmetric upon adsorption. The adsorption energy is 1.677 eV.

The pedestal and cave sites are "open" sites [Figs. 3(d) and 3(e)] and a direct adsorption of a molecule through one single atom pointing at the surface may be unfavorable. The adsorption energies on those two sites are indeed rather small compared to the other dissociative sites, i.e., 0.478 eV and 0.051 eV, respectively. There is no longer a direct Si-O bond, but the binding occurs through simultaneous weak interaction of the oxygen with four silicon atoms. The Si-O distance varies between 2.74 Å and 2.90 Å for the pedestal site and 3.40 Å and 3.79 Å for the cave site. As a result of the looser Si-O interaction, the C-O bond becomes shorter (1.34 Å for the pedestal site and 1.29 Å for the cave one). In both cases one dimer is unbuckled because of the binding with the H fragment, but no unbuckling is associated to the Si-phenoxy interactions.

In all cases no deformation of the phenoxy ring occurs upon adsorption. As for the hydrogen, regardless of the starting position, the final outcome is always on top of a silicon atom.

C. Phenoxy tilt and rotation—hydrogen position

Different conformations of the phenoxy fragment were evaluated for the adsorption on the top site, i.e., the 45° bent [Fig. 4(e)] on the surface and 90° rotated around the C-O bond [Fig. 4(b)]. For the latter conformation, the adsorption on either atom of a silicon dimer was calculated [Figs. 4(b)

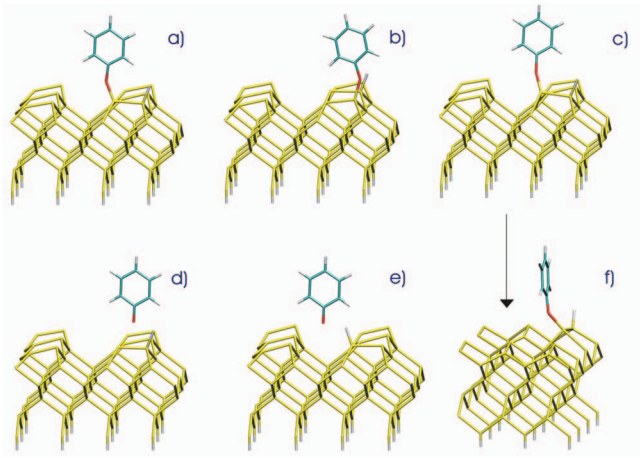

FIG. 3. (Color online) Optimized geometries of phenol dissociatively adsorbed on Si(100)2×1 surface sites. The models are ordered according to their increasing binding energy: (a) top site, (b) bridge site, (c) valley-bridge site, (d) pedestal site, (e) cave site. The model marked as (f) is the valley-bridge site plotted in a different perspective to show the phenol position between two dimer rows.

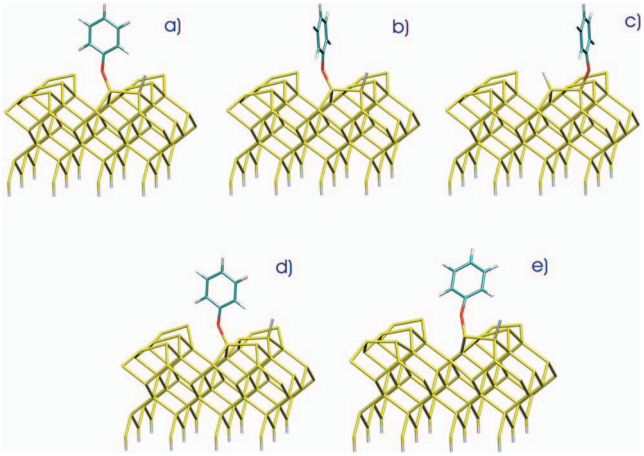

FIG. 4. (Color online) Various options of dissociative phenol adsorption on a top site: (a) standard adsorption of the phenoxy fragment, (b) the phenoxy fragment is 90° rotated along the C-O bond, (c) the rotated phenoxy fragment is initially placed on the up atom of the silicon dimer: the starting energy is higher compared to the previous model, but the final energy and geometry are quite similar, (d) phenoxy fragment and hydrogen are positioned on a neighboring silicon dimer, (e) the phenoxy fragment is bent 45° towards the surface.

and 4(c)], due to the nonequivalence of the up and the down atoms of the dimer in terms of hindrance and electronic density. Furthermore, we evaluated the effect of the hydrogen and phenoxy mutual positions, by placing the hydrogen on a neighboring dimer instead of the same dimer [Fig. 4(d)].

The dissociative top models are sketched in Fig. 4. The binding energies and geometrical parameters are reported in Tables I and II, respectively.

With the exception of the 45° bent model, in all other cases the main geometrical parameters, such as Si-O and O-C distances, as well as residual dimer buckling, are similar. The energy difference between the standard top position and the 90° rotated position is 0.038 eV, a negligible energy difference for the rotation around the vertical axes. No significant energy difference can be related to the binding of the phenoxy fragment to either atom of the silicon dimers (0.003 eV).

The positioning of the hydrogen fragment on a neighboring dimer, instead of the same dimer as the phenoxy fragment, is responsible for a lowering of the adsorption energy of 0.027 eV. This is also a negligible energy difference in terms of hydrogen migration on the surface, a process which was sometimes detected in cases of alcohol dissociative adsorption on Si(100)2×1.[6,26]

At variance with these findings, the bending of the phenoxy fragment on the surface is an unfavorable process. A 45° bending is associated to an energy loss of 1.004 eV with respect to the standard top site, and an increase of the Si-O-C angle to 156.9°.

D. Density maps

The electronic density was calculated for the optimized models of two representative molecular and two dissociative models in their local minimum structures and for the separate moieties (silicon surface and phenol molecule or phenoxy +hydrogen fragments). The positive and negative differences of the electronic densities were, then, plotted in Fig. 5.

The representative models are the top [Figs. 5(a) and 5(b)] and pedestal [Figs. 5(c) and 5(d)] ones in the dissociative group, i.e., with the phenoxy fragment pointing at a single silicon atom or equally distant from more silicon atoms and the bridge [Figs. 5(e) and 5(b)] and top [Figs. 5(g) and 5(h)] sites in the group of molecularly adsorbed phenol, i.e., a nonaromatic and an aromatic one.

The different electron density plots are reported for different values. The top dissociative, pedestal dissociative, and bridge molecular sites are plotted at the isosurface value of $\pm 2\times 10^{-3} el/\text{Å}^3$. The top molecular site is plotted for a much lower value, $\pm 5\times 10^{-4} el/\text{Å}^3$, since the weak interaction with the surface has a mild effect on the electronic rearrangement.

A different perspective has been chosen for the various models, in order to give a better view of the electron migration. In Fig. 5, we present the front view of the pedestal, top dissociative, and top molecular sites, and the side view of the bridge site.

The electron distribution of the top and pedestal dissociative sites is similar. We observe two main electron rearrangements: the first one in the bonding area between silicon and oxygen and silicon hydrogen; the second one is a rearrangement of the ring electrons. The bonding area between the surface and the fragments is characterized by an increase of density (red regions) at the expense of the surrounding areas (blue regions). Simultaneously, a small polarization occurs on the surface region underneath the silicon dimers involved in the adsorption (red and blue area). The oxygen atom of the phenoxy fragment is at the boundary between the positive and negative density in the binding region with the surface.

The bonds of the ring closer to the surface are also affected by the adsorption process, since they gain electron

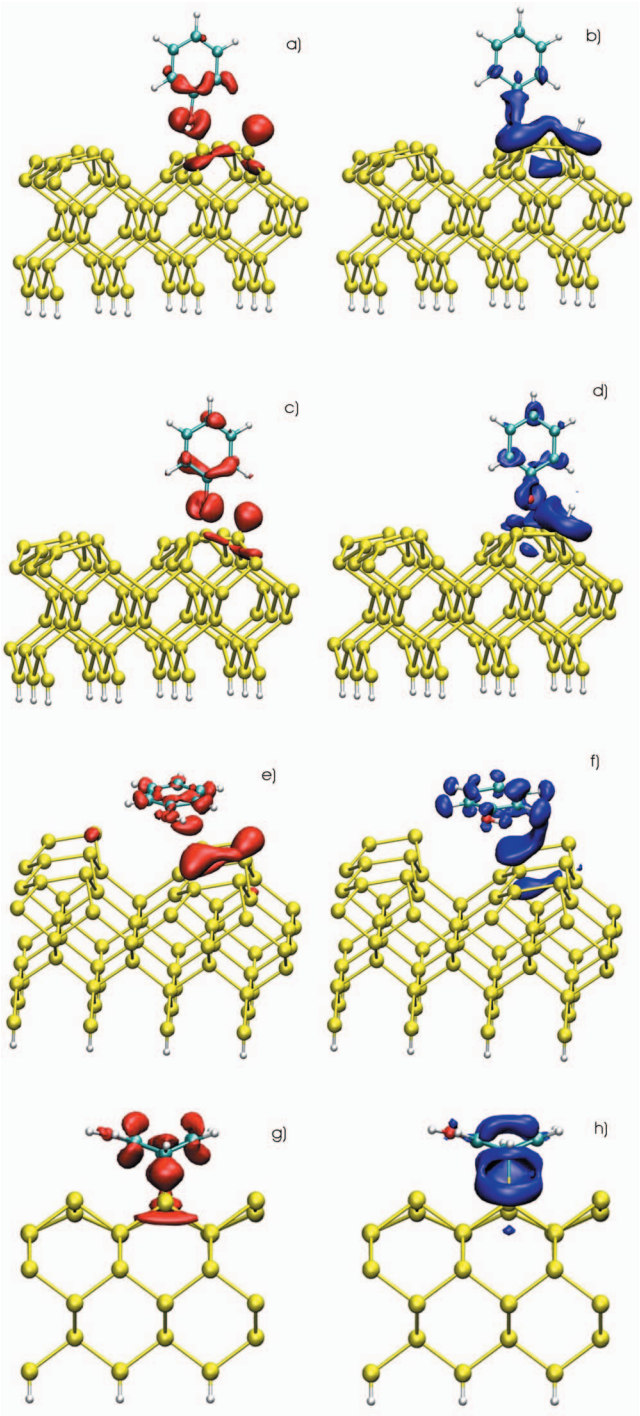

FIG. 5. (Color online) The positive and negative differences of the electronic densities.

density. Correspondingly, areas of electron loss are localized on the carbon atoms involved in the bonds.

The major differences between the top and the pedestal dissociative models are the larger rearrangements of the electron density of the surface and the more uniform electron redistribution of the ring electrons in the former compared to the latter case.

The top and bridge molecular adsorptions are quite different between them. The interaction between phenol and the surface in the top configuration is very weak and the electron density has been plotted for a value 4 times smaller than the other ones. We can observe a polarization of the silicon surface on the side closer to the phenol molecule and the simultaneous polarization electron density of the phenol ring.

The electron density redistribution of the phenol molecular adsorption on the bridge site is typical of a 1,4-cyclohexadiene. We clearly observe the increase of electron density between the carbon atoms 1-2 and 4-5 above and underneath the ring plane (electron density increase between alternative bonds). Simultaneously, the region above the carbon atoms 2 and 4 and symmetrically 5 and 1 is depleted. Finally, a large increase of density occurs in the region between the silicon and the carbon atoms involved in the binding process at the expense of the area around it.

E. Adsorption energy sequence and transition barrier

The ordering of the phenol adsorption sites according to their adsorption energy is $T_D > B_D > V_D > B_M > P_D > V_M > P_M > T_M > C_D > C_M$. The difference in adsorption energy between the most favorable dissociative (T_D) and molecular (B_M) site is 1.971 eV. Then, in an energy range of 0.478 eV we find the complete sequence from the bridge molecular to the cave dissociative. The molecular adsorption on the cave site is not stable (adsorption energy $=-0.494$ eV).

This sequence of binding energies gives an indication on the possibilities of dissociative vs molecular adsorption. The dissociative adsorption of phenol on the top site is the most favorable one and, whenever possible, the adsorption on different sites ends up in an on-top adsorption (bridge site). As far as molecular adsorption is concerned, there are two modalities of adsorption that may or may not break the aromatic character of the phenol ring. Different adsorption energies are associated to the molecular adsorption types. However, there is no clear-cut order between less favorable dissociative sites and the molecular sites.

We evaluated the kinetic aspects of the dissociative vs molecular adsorption process by calculating the minimum energy path that connects a chosen dissociative adsorbate to a suitable molecular one, in the hypothesis that the latter act as an adsorption precursor. The chosen connecting sites were the dissociative top site, i.e., the energetically most favored one and the molecular valley bridge, i.e., the one geometrically most similar to the dissociative site such that the calculated energy barrier can be mostly ascribed to the transformation process and not to pure geometrical rearrangements on the surface. We calculated the energy barrier by nudged elastic band, a technique that has proven to be very efficient to determine minimum energy paths in complex chemical reactions. Interestingly, we found an energy barrier <0.2 eV, hence lower than the thermodynamic energy of the adsorbate at room temperature. This implies that whenever phenol adsorbs molecularly on the valley-bridge site, it readily undergoes a transition to a dissociative top one.

Although calculated for one specific pathway only, such a small energy barrier allows us to consider the dissociative adsorption of phenol on Si(100)2×1 at low coverage the most favorable process, also according to kinetic considerations.

IV. CONCLUSIONS

We investigated the competitive adsorption of a bifunctional molecule, phenol, on Si(100)2×1 by first-principles calculations. We performed geometry optimizations of phenol adsorbed on five possible adsorption sites, both molecularly and dissociatively, in the low coverage regime. This theoretical investigation follows photoemission experiments performed on two silicon surfaces, the (111)7×7 (Ref. 27) and the (100)2×1,[26] where different adsorption types may be found depending on the coverage.

We find that the dissociative adsorption on top of the silicon dimer is the most favorable adsorption site, with a calculated adsorption energy of 2.560 eV. Furthermore, we found a very small energy difference for the rotation around the phenol axis and the adsorption on either atom of the silicon dimer. The 45° bend of the phenoxy fragment on the silicon plane, instead, results in a decrease of adsorption energy. The hydrogen migration on the silicon surface is energetically possible, since the energy difference associated to the hydrogen position on the same dimer as the phenoxy fragment or on the neighboring one is only 0.027 eV.

Within the group of dissociative adsorption the lowest energies are associated to output models mostly similar to an on-top site (starting bridge or valley bridge). The starting pedestal and cave site remain "open" sites and are characterized by higher energies.

In the molecular group, phenol on the bridge, valley-bridge, and pedestal sites gives rise to an adsorption through an addition reaction and subsequent removal of the aromatic character. The output geometries are standard bridge on a dimer or across two dimers, or a diagonal bridge, respectively. The interaction of nondissociated phenol on the top and cave sites occurs retaining the flat geometry and is characterized by a lower or negative binding energy.

When comparing the binding energies of the dissociative and the molecular groups between them, we find that the dissociative top site is the most favorable adsorption site and that the other sites are mixed according to the order $T_D > B_D > V_D > B_M > P_D > V_M > P_M > T_M > C_D > C_M$.

Different electron density maps were calculated for four representative adsorption models: molecular bridge (NA), molecular top (A), dissociative top, and dissociative pedestal.

The kinetic aspects of the dissociative adsorption were evaluated by calculating the minimum pathway that connects the valley-bridge molecular to the top dissociative adsorption site, by climbing image nudged elastic band. We found an energy barrier <0.2 eV, hence lower than the thermal vibration at room temperature.

ACKNOWLEDGMENTS

The authors wish to thank R. J. Bakker (PSI, Villigen, Switzerland) for software assistance and P. Cazzato (CASPUR, Rome, Italy) for helpful discussions.

[1] E. I. Dimitriadis, D. Girinoudi, A. Thanailakis, and N. Georgoulas, Semicond. Sci. Technol. **10**, 523 (1995).
[2] M. Ikeda, M. Inayoshi, and A. Hiraya, J. Vac. Sci. Technol. A **16**, 2252 (1998).
[3] C. Huang, W. Widdra, and W. H. Weinberg, Surf. Sci. **312**, L953 (1994).
[4] S.-Y. Chu and A. B. Andersson, Surf. Sci. **194**, 55 (1988).
[5] A. J. Dyson and P. V. Smith, Surf. Sci. **375**, 45 (1997).
[6] M. Carbone, M. N. Piancastelli, R. Zanoni, G. Comtet, G. Dujardin, and L. Hellner, Surf. Sci. **390**, 219 (1997).
[7] J. Eng, K. Raghavachari, L. M. Struck, Y. J. Chabal, B. E. Bent, G. W. Flynn, S. B. Christman, Ed. E. Chaban, G. P. Williams, K. Radermacher, and S. Mantl, J. Chem. Phys. **106**, 9889 (1997).
[8] M. Carbone, M. N. Piancastelli, J. J. Paggel, Chr. Weindel, and K. Horn, Surf. Sci. **412**, 441 (1998).
[9] F. Tao, Z. L. Yuan, X. F. Chen, Z. H. Wang, Y. J. Dai, H. G. Huang, and G. Q. Xu, Phys. Rev. B **67**, 245406 (2003).
[10] M. Carbone, M. N. Piancastelli, M. P. Casaletto, R. Zanoni, G. Comtet, G. Dujardin, and L. Hellner, Surf. Sci. **498**, 186 (2002).
[11] M. Toscano and N. Russo, J. Mol. Catal. **55**, 101 (1989).
[12] B. I. Craig and P. V. Smith, Surf. Sci. **276**, 174 (1992).
[13] B. I. Craig, Surf. Sci. **298**, 87 (1993).
[14] B. Weiner, C. S. Carmer, and M. Frenklach, Phys. Rev. B **43**, 1678 (1991).
[15] A. J. Fisher, P. E. Blöchl, and G. A. D. Briggs, Surf. Sci. **374**, 298 (1997).
[16] M. Preuss, W. G. Schmidt, K. Seino, and F. Bechstedt, Appl. Surf. Sci. **234**, 155 (2004).
[17] X. Lu, Q. Zhang, and M. C. Lin, Phys. Chem. Chem. Phys. **3**, 2156 (2001).
[18] P. L. Silvestrelli, Surf. Sci. **552**, 17 (2004).
[19] P. L. Silvestrelli, O. Pulci, M. Palummo, R. Del Sole, and F. Ancillotto, Phys. Rev. B **68**, 235306 (2003).
[20] I. D. Petsalakis, J. C. Polanyi, and G. Thoedorakopoulos, Surf. Sci. **544**, 162 (2003).
[21] M. Carbone and K. Larsson, J. Phys.: Condens. Matter **17**, 1289 (2005).
[22] M. Carbone, G. Comtet, G. Dujardin, L. Hellner, and A. J. Mayne, J. Chem. Phys. **117**, 5012 (2002).
[23] B. Borovsky, M. Krueger, and E. Ganz, J. Vac. Sci. Technol. B **17**, 17 (1999).
[24] F. Costanzo, C. Sbraccia, P. L. Silvestrelli, and F. Ancilotto, Surf. Sci. **566-568**, 971 (2004).
[25] F. Y. Naumkin, J. C. Polanyi, and D. Rogers, Surf. Sci. **547**, 335 (2003).
[26] M. P. Casaletto, M. Carbone, M. N. Piancastelli, K. Horn, K. Weiss, and R. Zanoni, Surf. Sci. **582**, 42 (2005).
[27] M. Carbone, M. N. Piancastelli, M. P. Casaletto, R. Zanoni, M. J. Besnard-Ramage, G. Comtet, G. Dujardin, and L. Hellner, Surf. Sci. **419**, 114 (1999).
[28] A. D. Becke, Phys. Rev. A **38**, 3098 (1988); C. Lee, W. Yang, and R. G. Parr, Phys. Rev. B **37**, 785 (1988).
[29] CPMD, Copyright IBM Corp. 1990–2006, Copyright MPI für Festkörperforschung Stuttgart 1997–2001.

[30] S. Baroni, A. Dal Corso, S. de Gironcoli, P. Giannozzi, C. Cavazzoni, G. Ballabio, S. Scandolo, G. Chiarotti, P. Focher, A. Pasquarello, K. Laasonen, A. Trave, R. Car, N. Marzari, and A. Kokalj, http://www.pwscf.org/

[31] D. C. Sorescu and K. D. Jordan, J. Phys. Chem. B **104**, 8259 (2000).

[32] P. Natchigall, K. D. Jordan, A. Smith, and H. Jónsson, J. Chem. Phys. **104**, 148 (1996).

[33] N. Troullier and J. L. Martins, Phys. Rev. B **43**, 1993 (1991).

[34] M. Carbone, A. Palma, and R. Caminiti, Phys. Rev. B **75**, 245332 (2007).

[35] T. A. Gadosy and R. A. McClelland, J. Mol. Struct.: THEOCHEM **369**, 1 (1996).

[36] P. Krüger and J. Pollmann, Phys. Rev. Lett. **74**, 1155 (1995).

[37] B. Borovsky, M. Krüger and E. Ganz, J. Vac. Sci. Technol. B **17**, 17 (1999).

[38] W. Humphrey, A. Dalke, and K. Schulten, J. Mol. Graphics **14**, 33 (1996).